Exploring Renner-Teller induced quenching in the reaction $H(^2S)+NH(a\,^1\Delta)$: A combined experimental and theoretical study

L. Adam and W. Hack[a)]
Max-Planck-Institut für Biophysikalische Chemie, D-37077 Göttingen, Germany

G. C. McBane[b)]
Department of Chemistry, Grand Valley State University, Allendale, Michigan 49401

H. Zhu,[c)] Z.-W. Qu,[d)] and R. Schinke[e)]
Max-Planck-Institut für Dynamik und Selbstorganisation, D-37073 Göttingen, Germany

(Received 11 October 2006; accepted 20 November 2006; published online 17 January 2007)

Experimental rate coefficients for the removal of $NH(a\,^1\Delta)$ and $ND(a\,^1\Delta)$ in collisions with H and D atoms are presented; all four isotope combinations are considered: NH+H, NH+D, ND+H, and ND+D. The experiments were performed in a quasistatic laser-flash photolysis/laser-induced fluorescence system at low pressures. $NH(a\,^1\Delta)$ and $ND(a\,^1\Delta)$ were generated by photolysis of HN_3 and DN_3, respectively. The total removal rate coefficients at room temperature are in the range of $(3-5)\times10^{13}$ cm^3 mol^{-1} s^{-1}. For two isotope combinations, NH+H and NH+D, quenching rate coefficients for the production of $NH(X\,^3\Sigma^-)$ or $ND(X\,^3\Sigma^-)$ were also determined; they are in the range of 1×10^{13} cm^3 mol^{-1} s^{-1}. The quenching rate coefficients directly reflect the strength of the Renner-Teller coupling between the $^2A''$ and $^2A'$ electronic states near linearity and so can be used to test theoretical models for describing this nonadiabatic process. The title reaction was modeled with a simple surface-hopping approach including a single parameter, which was adjusted to reproduce the quenching rate for NH+H; the same parameter value was used for all isotope combinations. The agreement with the measured total removal rate is good for all but one isotope combination. However, the quenching rates for the NH+D combination are only in fair (factor of 2) agreement with the corresponding measured data. © *2007 American Institute of Physics*. [DOI: 10.1063/1.2409926]

I. INTRODUCTION

Transitions between adiabatic electronic states are an important aspect of bimolecular chemical reactions. They can be induced by various coupling schemes. One example is the coupling between electronic rotation and bending vibration, which is known as the Renner-Teller (RT) effect.[1–3] The resulting splitting of a degenerate electronic state upon bending of a linear molecule was first observed experimentally in NH_2.[4] The spectroscopy of NH_2 has received intense theoretical and experimental scrutiny since then.[5–8] Collision complexes formed during bimolecular reactions generally have much higher energies than initial states in spectroscopy, so RT coupling may have more dramatic effects on reaction product distributions. The role of RT coupling in a reaction that passes through the NH_2 complex is the subject of this paper.

The reaction

$$N(^2D)+H_2(X\,^1\Sigma_g^+)\xrightarrow{k_1}H(^2S)+NH(X\,^3\Sigma^-) \quad (1)$$

has recently been studied in great detail. It proceeds over a small barrier and through the deep potential well of the $NH_2(\tilde{X}\,^2A'')$ ground state potential energy surface (PES) and is exothermic by more than an eV (see Fig. 1). Accurate global PESs have been constructed from electronic structure calculations for the ground as well as excited states.[9–14] Numerous classical and quantum mechanical dynamics calculations have been performed on these PESs, and the theoretical results have been compared with experimental data on a detailed level.[9–11,15–21]

For example, Lin and Guo computed rate coefficients by exact quantum dynamics[20] on an accurate PES.[11] Their calculated rates were slightly higher than the experimental results of Suzuki *et al.*[22] The small disagreement may be due to an underestimation of the reaction barrier; a more recent PES of the ground electronic state[14] has a barrier which is higher by 13% (0.0946 eV vs 0.0835 eV). Another recent quantum mechanical study by Chu *et al.*,[21] using the *J*-shifting approximation and the PES of Varandas and Poveda,[23] yielded even better agreement with experiment; the calculated rate coefficients are marginally smaller than the experimental results. In both investigations only reactions in the $\tilde{X}\,^2A''$ ground state were considered.

However, the $\tilde{X}\,^2A''$ ground state of NH_2 (termed *X* in

[a)]Electronic mail: whack@gwdg.de
[b)]Electronic mail: mcbaneg@gvsu.edu
[c)]Present address: Institut für Physik, Humboldt-Universität zu Berlin, Newtonstrasse 15, D-12489 Berlin, Germany.
[d)]Present address: Leids Instituut voor Chemisch Onderzoek, Gorlaeus Laboratoria, Universiteit Leiden, Postbus 9502, 2300 RA Leiden, The Netherlands.
[e)]Electronic mail: rschink@gwdg.de

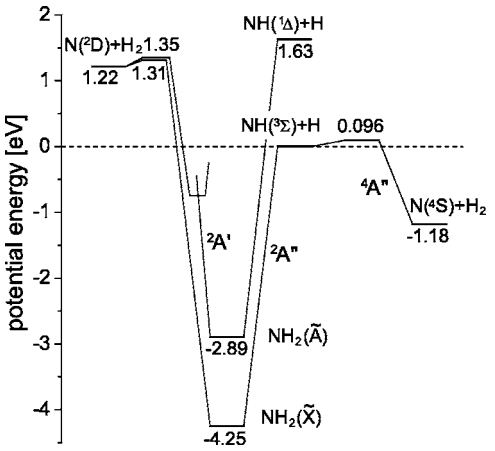

FIG. 1. Schematic energy level and correlation diagram for the reactions $NH(X\,^3\Sigma^-)+H(^2S)\rightarrow$ products and $NH(a\,^1\Delta)+H(^2S)\rightarrow$products. Energies are given in eV. Reprinted, with permission of The American Institute of Physics, from Ref. 14.

what follows) forms a RT pair with the first excited state $\tilde{A}\,^2A'$ (termed A); that is, the two states are degenerate at linear geometries. The RT coupling may significantly affect the reactivity of reaction (1) by transitions from the A PES—which initially is also accessed by the reactants—to the X PES inside the highly excited NH_2 complex and subsequent fragmentation to $NH(^3\Sigma^-)$ products. The reaction barrier in the entrance channel of the A state is only slightly higher than the barrier of the X state and therefore complex formation should be comparable on both PESs. It is therefore possible that the good agreement obtained in the one-state quantum calculations is only fortuitous.

Santoro *et al.*[24] investigated the influence of RT coupling in reaction (1) by means of a surface-hopping trajectory approach. They concluded that the inclusion of both electronic states and the RT coupling between them affects the integral cross section for reaction (1) only slightly [Fig. 3(c) in Ref. 24]. The reaction cross section for $^2A'$ as an initial electronic state is of the order of 1 Å^2 at the maximum at about 10 kcal/mol. Recently, Defazio and Petrongolo[25] investigated the same problem with a fully quantum mechanical approach. In contrast to the trajectory study, these authors found a large reaction cross section for wave packets starting on the A PES (about 4.5 Å^2 at 10 kcal/mol); it is roughly half the cross section for wave packets starting in the X ground state. The calculated rate coefficient, summed over both electronic states, is markedly smaller than the experimental one, which the authors attribute to an overestimation of the barrier of the PES used in their calculations (0.099 eV).[9,10] Shifting the cross sections by 0.0156 eV to lower collision energies yielded good agreement with the experimental results.[25]

However, in view of these three most recent theoretical investigations[20,21,25] of reaction (1) and the comparison of calculated and measured rate coefficients, it is still not clear whether or not RT coupling is important in NH_2 complexes at total energies high above the barrier to linearity.

In this study we present experimental results that are directly related to the strength of the RT coupling: the quenching of excited $NH(a\,^1\Delta)$ in collisions with H. This process starts in the excited state, and the $NH(X\,^3\Sigma^-)$ ground state radicals can be produced only by RT transitions from $^2A'$ to $^2A''$ (Fig. 1). In particular, we present rate coefficients for the removal of $NH(a)$ in the reaction

$$NH(a\,^1\Delta)+H(^2S)\xrightarrow{k_{NH+H}}\text{products} \tag{2}$$

and all other possible isotope combinations: $ND(a)+D$, $NH(a)+D$, and $ND(a)+H$.

Reaction (2) comprises five different reaction paths. For the isotope substituted reaction,

$$NH(a\,^1\Delta)+D(^2S)\xrightarrow{k_{NH+D}}\text{products}, \tag{3}$$

they are (see Fig. 1)

$$NH(a)+D\rightarrow NH(a)+D \tag{3a}$$

$$\xrightarrow{k^e_{NH+D}} ND(a)+H \tag{3b}$$

$$\xrightarrow{k^q_{NH+D}} NH(X)+D+1.63\ \text{eV} \tag{3c}$$

$$\xrightarrow{k^{e+q}_{NH+D}} ND(X)+H+1.63\ \text{eV} \tag{3d}$$

$$\xrightarrow{k_{NH+D\rightarrow N+HD}} N(^2D)+HD+0.41\ \text{eV}, \tag{3e}$$

where the exothermicities are taken from our electronic structure calculations (without zero-point energies). Channels (3a) and (3b) represent inelastic scattering and atom-exchange reactions. They can proceed exclusively on the excited-state PES without RT transitions. Channels (3c) and (3d) illustrate the quenching of $NH(a)$ without and with H/D atom exchange, respectively; they are exothermic by 1.63 eV. Finally, the exothermic channel (3e) can be accessed on both PESs. The product channel $N(^4S)+HD$ is spin forbidden under single collision conditions; we will not consider it in discussions of the complex dynamics, though we do include secondary reactions producing $N(^4S)$ in our experimental data analysis.

The considerable number of reaction possibilities for the four isotope combinations requires a detailed terminology. In the following, e and q stand for "exchange" and "quenching," respectively. For example, k^{e+q}_{ND+H} is the rate coefficient for reaction $ND(a)+H\rightarrow NH(X)+D$.

In the experiment we not only measure the total removal rate coefficient k_{NH+D}, but also determine the individual rate coefficients for the production of $NH(X)$ and $ND(X)$, i.e., the rate coefficients k^q_{NH+D} and k^{e+q}_{NH+D}. The latter two reflect the RT coupling strength directly. If the RT coupling were very weak, the production of $NH(X)$ or $ND(X)$ would be small. On the other hand, if the RT interaction were very strong, k^q_{NH+D} and k^{e+q}_{NH+D} would govern the total removal rate. Once the molecule is in the electronic ground state dissociation is very fast because of the large exothermicity. For the reactions $NH(a)+H$ and $ND(a)+D$ the pure exchange channels do not contribute to the removal of $NH(a)$ or $ND(a)$, respec-

tively; therefore the removal rate coefficients are smaller than those for the reactions with different hydrogen isotopes.

The experimental results are accompanied by classical trajectory calculations employing the surface-hopping method of Santoro *et al.*[24] to the quenching of NH(a) in collisions with hydrogen atoms. The computed rate coefficients can be unambiguously compared with the measured data. When the expression for the semiclassical transition probability given by Santoro *et al.*[24] [Santoro-Petrongolo-Schatz (SPS)] is used, the pure quenching rate coefficients are much too small. A reanalysis of the derivation of the essential equations leads us to believe that the SPS expression is missing an important term. However, calculations using an expression we think is more appropriate yield quenching rate coefficients that are much too large compared to the experimental results. We argue that the inappropriateness of classical mechanics near the turning point for the bending motion in the vicinity of linearity causes this deficiency. Finally, we use a very simple surface-hopping model including a single adjustable parameter—the same for all isotope combinations—to describe the RT coupling and calculate the various rate coefficients.

The removal of $NH(X\,^3\Sigma^-)$ in collisions with H and D atoms was previously studied by Adam *et al.*[13] and Qu *et al.*,[14] respectively. Classical trajectory calculations on the $^4A''$ PES and the $^2A''$ PES were in satisfactory agreement with the experimental data.

II. EXPERIMENT

A. Experimental setup

The experimental setup is described in detail elsewhere,[26] and only the essentials are repeated here. The measurements were performed at room temperature (298 K) in a quasistatic laser-flash photolysis/laser-induced fluorescence (LIF) system. "Quasistatic" means that the flow through the reaction cell is negligible between the pump and the probe pulses but sufficient to exchange the gas volume between two subsequent pump pulses and to transport the H/D atoms (see below). The carrier gas was He at a total pressure in the range of 5–7 mbar in most cases. For the photolysis, a XeCl exciplex laser (Lambda Physik LPX 205) with pulse energies in the range of 200–400 mJ and a beam area of about 1.1 cm^2 was used. It runs at a repetition rate of 10 Hz. The probe laser was a dye laser (Lambda Physik FL 3002) with a beam area of 7 mm^2. It was pumped by an exciplex laser (Lambda Physik LPX 205, XeCl; 230–290 mJ). The NH(a) radicals were produced by HN_3 photolysis in the $\tilde{A}-\tilde{X}$ band at $\lambda=308$ nm. The ND(a) radicals were produced by photolyzing a mixture of DN_3 and HN_3 at the same wavelength. The NH(a) radicals were detected by undispersed fluorescence following the excitation of the P_3 line of the transition of $NH(c\,^1\Pi,v=0)\leftarrow(a\,^1\Delta,v=0)$ at $\lambda=326.22$ nm, and the ND(a) radicals were detected via the P_4 line of that transition at $\lambda=324.94$ nm. $NH(X,v=0)$ was detected after excitation of the $P_2(2)$ line at $\lambda=336.48$ nm of the transition $NH(A\,^3\Pi,v=0)\leftarrow(X\,^3\Sigma,v=0)$. The undispersed fluorescence from the excited state was observed in the wavelength range of 325–328 nm perpendicular to the laser beam using a long pass filter (KV370, Schott) or an interference filter 326.3 nm (Schott) to suppress scattered radiation from the excitation beam. ND(X) was detected at $\lambda=336.38$ nm via the $P_1(4)$ line of the transition $ND(A\,^3\Pi,v=0)\leftarrow(X\,^3\Sigma^-,v=0)$.

The H (D) atoms were generated in a side arm of the reactor in a microwave discharge of a H_2/He (D_2/He) mixture (5% mole fraction H_2 or D_2 in He). The absolute initial atom concentration was determined by titration with NO_2 via the reaction $H(D)+NO_2\rightarrow OH(OD)+NO$. The increase of OH (OD) with increasing NO_2 was observed by LIF. The OH was detected via the $Q_1(2)$ line of the transition $OH(A\,^2\Sigma^+,v=0)\leftarrow(X\,^2\Pi,v=0)$ at $\lambda=308.01$ nm ($\lambda=307.54$ nm for OD) with a dye laser (Lambda Physik LPD 3002) pumped by a neodymium-doped yttrium aluminum garnet laser (Spectra Physics GC-R-3-10).

The NH(X) concentration produced in the fast quenching reaction

$$NH(a\,^1\Delta)+Xe\rightarrow NH(X\,^3\Sigma^-)+Xe \tag{4}$$

was also measured in some control experiments. In those experiments quenching of the $NH(A\,^3\Pi)$ state (i.e., the upper state used in the LIF measurements) by Xe could introduce a systematic error. We confirmed that addition of more Xe than needed to quench NH(a) did not change the NH(X) LIF signal. Thus, the NH(X) LIF signals in the absence and presence of Xe could be compared directly.

HN_3 (DN_3) and Xe were added to the reactor via an inner probe which ended 1 cm above the photolysis volume. The NO_2 for the titration was also added to the system through this probe. To improve the mixing, a second He flow was added in both cases (HN_3/Xe or NO_2). The distance between the entrance of HN_3 (DN_3) and the photolysis volume was kept as small as possible to minimize the dark reaction of H atoms with HN_3 (see below). A distance of about 1 cm was found to be the optimum for mixing on one hand and limiting the dark reaction on the other.

Gases with the highest commercially available purity were used: He, 99.9999%, Praxair; Xe, 99.998%, Messer-Griesheim; N_2, 99.995%, UCAR; NO_2, 99.5%, Merck; H_2, 99.999%, Praxair; and D_2, 99.7% (the remainder H_2), Messer-Griesheim. HN_3 was synthesized by melting stearic acid, $CH_3(CH_2)_{16}COOH$ (97.0%, Merck), with NaN_3 (99.0%, Merck). It was dried with $CaCl_2$ and stored in a bulb at partial pressures $\leqslant$200 mbar diluted with He (overall pressure approximately 1 bar). For safety reasons, the HN_3 containing devices were covered with a wooden box since HN_3 is highly explosive even at low pressures. The DN_3 was obtained by adding D_2O into the storage bulb. The resulting HN_3/DN_3 mixture had mole fractions x_{HN_3} and x_{DN_3} of about 0.5.

B. Experimental results

Experiments were performed for all four possible isotope combinations: NH+H, ND+D, NH+D, and ND+H. The detailed data from the various experiments (pressures, concentrations, rate coefficients, etc.) are available in the

TABLE I. Measured and calculated rate coefficients at 298 K (in units of 10^{12} cm^3 mol^{-1} s^{-1}) and fraction of the product channels (in%), respectively.

Reaction	Notation	Rate coefficients	
		Measured	Calculated
NH(a)+H→products	k_{NH+H}	29±10	27.8
→NH(X)+H	k^q_{NH+H}	10 (35%)	9.9 (36%) (*)
ND(a)+D→products	k_{ND+D}	28±9	26.6
NH(a)+D→products	k_{NH+D}	50±14	33.6
→NH(X)+D	k^q_{NH+D}	8.5 (17%)	4.4 (13%)
→ND(X)+H	k^{e+q}_{NH+D}	7.5 (15%)	3.2 (9%)
→ND(a)+H	k^e_{NH+D}	8.0 (16%)	13.4 (40%)
ND(a)+H→products	k_{ND+H}	49±10	46.6

supplementary electronic material.[27] All measured (and calculated) rate coefficients are summarized in Table I.

The depletion of NH($a\,^1\Delta$) via reaction (2) was measured under pseudo-first-order conditions, i.e., $[NH(a)]_0 \ll [H(^2S)]_0$. Typical NH(a) concentration profiles in the absence and in the presence of H atoms are shown in Fig. 2. NH(a) is formed at $t=0$ by the photolysis pulse. From the slopes of ln[NH(a)] versus time first order rate coefficients k_+ and k_- were determined. The rate coefficient k_{eff} was then obtained as the difference of these two rates. The second order rate coefficient is given by $k_{NH+H}=k_{eff}/[H]$.

The NH(a) depletion in the absence of H atoms is mainly due to the reaction with the precursor molecule HN_3. The reaction of NH(a) with H_2 at the given H_2 concentration contributes about 10% of the first order rate in the absence of H atoms. (The rate coefficient for the quenching reaction NH(a)+H_2 was measured by Tezaki *et al.*[28] and has the value 2.5×10^{12} cm^3 mol^{-1} s^{-1}.)

The rate measurements were performed in a narrow pressure range (total pressure $p=5-7$ mbar), and the H atom concentration [H] was in the range of $(1.5-6.8)\times10^{-11}$ mol cm^{-3}. It was not possible to vary [H] over a wider range, and therefore the variation of the first order rate constant with [H] could not be investigated. The final rate coefficient reported in Table I was obtained as the average of 20 different measurements (see Table I of the supplementary electronic material[27]). The large uncertainty is mainly due to the uncertainty in the H atom concentration and the scatter in the first order rate constant.

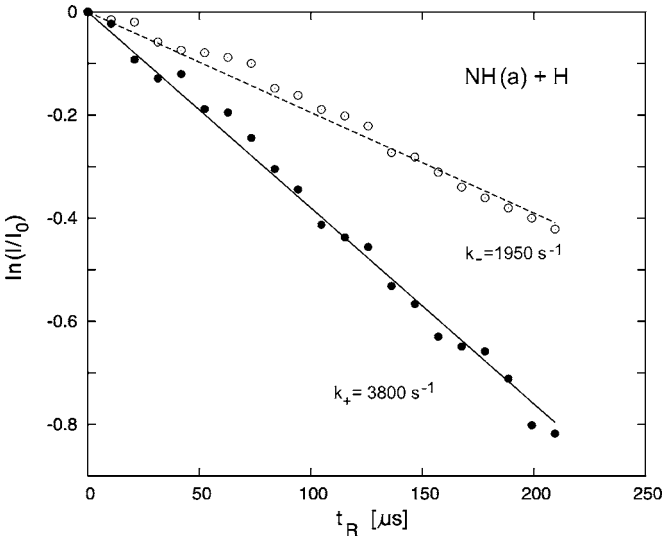

FIG. 2. NH(a) concentration as a function of time for the reaction NH(a)+H→products. t_R is the time between photolysis and analysis laser. I and I_0 are the NH(a) fluorescence signals at t_R and $t_R=0$. The open circles (○) are taken with discharge off and the full dots (●) are taken with discharge on. The total pressure is $p=7.1$ mbar and $[H]_0=5.5\times10^{-11}$ mol cm^{-3}. The difference of the slopes, k_+-k_-, yields the first order rate coefficient.

In order to determine the contributions of the quenching channel yielding NH(X) to the overall NH(a) depletion, the NH(X) concentrations produced in reaction (2) were compared at a long pump-probe delay time to those produced in the fast quenching reaction (4), for which a rate constant $k=5.8\times10^{12}$ cm^3 mol^{-1} s^{-1} is known.[26] The NH(X) concentrations were measured at the maxima of the NH(X) temporal profiles (more details are given in Table II of the supplementary electronic material[27]).

When H atoms are present, the experiment is complicated by a background concentration of NH(X) that is independent of time. It is due to the dark reaction of H atoms with the precursor molecule HN_3 according to[29]

$$2H + HN_3 \rightarrow H_2 + NH(X) + N_2. \quad (5)$$

In order to minimize the NH(X) background, the distance between the end of the HN_3 admixing probe and the laser photolysis volume, i.e., the time in which the dark reaction can occur, should be kept as short as possible. It is limited, however, by the time required to mix HN_3 thoroughly into the flow because it is necessary to photolyze a homogeneous mixture. Thus, a NH(X) background, $[NH(X)]_\infty$, independent of the reaction time (i.e., the time between photolysis and analysis pulse) was unavoidable and had to be subtracted from the signal. The NH(X) LIF signal from $[NH(X)]_\infty$, published electronically,[27] was about 80% of the signal of NH(X) due to the quenching channel in the reaction NH(a)+H. This large correction gave rise to a significant uncertainty in the determination of the quenching rate constant. The NH(X) concentration also had to be corrected for the consumption of NH(X) in reactions with H atoms, i.e., the reaction NH($X\,^3\Sigma^-$)+H→products. This correction was done by simulation of the system with the known rate constant of 1.9×10^{12} cm^3 mol^{-1} s^{-1} measured by Adam *et al.*[13] Finally, the contribution of quenching to the overall loss rate of NH(a) was found to be (35±7)% and the corresponding rate coefficient is given in Table I.

The rate constant for the isotope substituted reaction

$$ND(a\,^1\Delta) + D(^2S) \xrightarrow{k_{ND+D}} \text{products} \quad (6)$$

was also measured under pseudo-first-order conditions, i.e., $[ND(a)]_0 \ll [D]_0$. The ND(a) temporal profile was measured with the discharge on and off under identical conditions otherwise, in analogy to Fig. 2. The D atom concentration was varied in the range of $(1.3-2.7)\times10^{-10}$ mol cm^{-3}, and the rates were determined at 7 and 14 mbar (Table III of the supplementary electronic material[27]). The rates obtained at a higher pressure, 2.1×10^{13} cm^3 mol^{-1} s^{-1}, seem to be slightly smaller than those at a lower pressure,

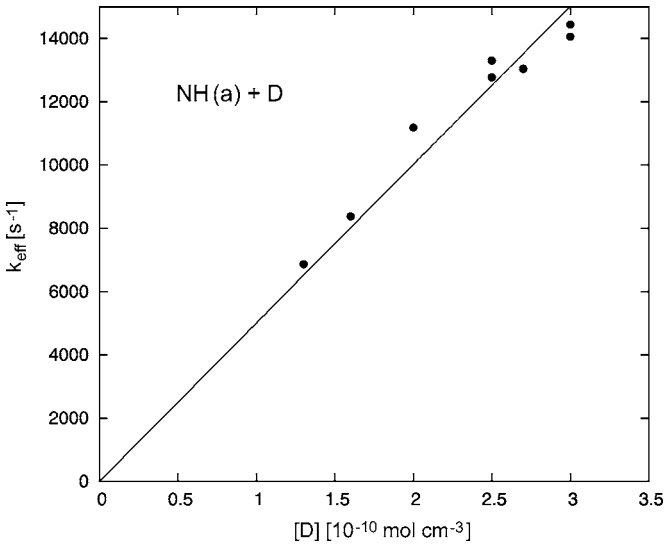

FIG. 3. First order rate coefficient vs D atom concentration in the reaction NH(a)+D→ products. The total pressure is p=7 mbars. The slope yields the second order rate coefficient.

2.9×10^{13} cm^3 mol^{-1} s^{-1}. We do not, however, consider this difference significant and simply averaged over all measurements. The final value (Table I) is, within the quoted error limits, the same as the rate coefficient measured for reaction NH(a)+H.

Reactions in which one H atom is substituted by a D atom are particularly interesting because the exchange pathway in the excited electronic state also contributes to the products. For reaction (3), i.e.,

$$\mathrm{NH}(a\,^1\Delta) + \mathrm{D}(^2S) \xrightarrow{k_{\mathrm{NH+D}}} \text{products},$$

the D atom concentration was varied in the range of $(1.3-3.0)\times10^{-10}$ mol cm^{-3} and the first order rate constants k_{eff} are shown in Fig. 3 (see also Table IV of the supplementary electronic material[27]).The rate coefficient was obtained from the slope of the straight line that goes through the origin and is given in Table I. It is significantly higher than $k_{\mathrm{NH+H}}$ since the exchange pathway [Eq. (3b)],

$$\mathrm{NH}(a\,^1\Delta) + \mathrm{D}(^2S) \xrightarrow{k^e_{\mathrm{NH+D}}} \mathrm{ND}(a\,^1\Delta) + \mathrm{H}(^2S),$$

also contributes to the total removal rate. A similar exchange of H atoms is also present in the reaction NH(a)+H, but does not contribute to $k_{\mathrm{NH+H}}$ because the reactant and product diatoms are identical.

The rate coefficient for the quenching pathway [Eq. (3c)],

$$\mathrm{NH}(a\,^1\Delta) + \mathrm{D}(^2S) \xrightarrow{k^q_{\mathrm{NH+D}}} \mathrm{NH}(X) + \mathrm{D}(^2S),$$

was obtained by comparison of the NH(X) formed in the reaction NH(a)+D with the NH(X) formed in the fast quenching reaction with Xe [Eq. (4)]. The supplementary material gives details of the analysis (Table V).[27] Likewise, the rate for the combined exchange and quenching channel [Eq. (3d)],

$$\mathrm{NH}(a\,^1\Delta) + \mathrm{D}(^2S) \xrightarrow{k^{e+q}_{\mathrm{NH+D}}} \mathrm{ND}(X) + \mathrm{H}(^2S),$$

was obtained from a computer simulation of the measured ND(X) concentration profile. The overall quenching channel, i.e., the sum of NH(X) and ND(X) formation, contributes 32% of the NH(a) consumption, 17% for NH(X) and 15% for ND(X). The corresponding rate coefficients are given in Table I.

With these data in hand, we can also consider the exchange reaction without quenching [Eq. (3b)]. To obtain the rate coefficient $k^e_{\mathrm{NH+D}}$ the measured ND(a) concentration profile was simulated using the rate coefficients $k_{\mathrm{NH+H}}$, $k^q_{\mathrm{NH+H}}$, $k_{\mathrm{NH+D}}$, $k^q_{\mathrm{NH+D}}$, and $k^{q+e}_{\mathrm{NH+D}}$, as well as those for the reactions NH($X\,^3\Sigma^-$)+H→products and NH($X\,^3\Sigma^-$)+D →products measured previously.[13,14] The initial NH(a) concentration was determined from the absorption through HN_3, i.e., the HN_3 concentration and the photolysis assuming a quantum yield of 1. With an absorption coefficient[30] $\epsilon(308\ \mathrm{nm})=4.15\times10^{-21}$ cm^2 the fraction of HN_3 photolyzed is about 0.1%. The initial NH(a) concentration was the weakest parameter in the simulation. The rate coefficient for exchange in the excited electronic state is of the same order as the individual quenching rate coefficients (Table I).

Finally, the reaction

$$\mathrm{ND}(a\,^1\Delta) + \mathrm{H}(^2S) \xrightarrow{k_{\mathrm{ND+H}}} \text{products} \qquad (7)$$

was considered. The H atom concentration was varied in the range of $(2.8-8.4)\times10^{-11}$ mol cm^{-3}, and the DN_3/HN_3 ratio was estimated from the NH(a)/ND(a) signals in the absence of H atoms. The rate coefficient obtained from four measurements (see Table VI of the supplementary electronic material[27]) is given in Table I. Since ND(a) and NH(a) are both present from the photolysis, measurements of isotope exchange reactions were not attempted.

III. CALCULATIONS

The quenching of NH($a\,^1\Delta$) by H atoms is the result of RT coupling between the lowest states with $^2A'$ and $^2A''$ symmetries, i.e., 1 $^2A'$ and 1 $^2A''$. In principle the second $^2A'$ state, 2 $^2A'$, could also be involved in reaction (3). 1 $^1A'$ and 2 $^2A'$ have a conical intersection (CI) in the collinear configuration at intermediate H–NH separations (see Fig. 3 of Ref. 14) and another CI near the N+H_2 channel for C_{2v} geometries (see Figs. 5 and 7 of Ref. 14). More detailed discussions of these CIs, including the nonadiabatic coupling elements, were provided by Vibók *et al.*[31] and Halász *et al.*[32] Takayanagi *et al.*[33] gave a detailed correlation diagram including all three states. We do not expect either CI to have a sizable effect on the quenching process. First, the CI in HNH geometries is in a position that is hard for the trajectories to reach; it is very near the total available energy, at a maximum on a long, narrow ridge along linear geometries. Second, the adiabatic PES of state 2 $^2A'$ is bound for the total energies involved in the present experiment (see Fig. 1 of Takayanagi *et al.*[33]). Trajectories that cross from 1 $^2A'$ to 2 $^2A'$ by nonadiabatic coupling at either CI must return eventually to the lower $^2A'$ PES. Therefore, it seems reasonable

to include only the ground state and the lowest *adiabatic* $^2A'$ PES in order to study the quenching of NH(a). This two-state model is the basis for the theoretical approaches presented here.

A. Santoro-Petrongolo-Schatz (SPS) model

We first implemented the trajectory surface-hopping model of Santoro *et al.*,[24] which is based on the "molecular dynamics with quantum transitions" or "fewest-switches" approach of Tully.[34] The nuclei follow a classical trajectory on either the A'' or the A' PES, and simultaneously an electronic wave packet in a two-state basis is propagated along the trajectory according to

$$\frac{dC_X}{dt} = \frac{-d\boldsymbol{Q}}{dt} \cdot \boldsymbol{d}_{XA} C_A \exp\left(\frac{-i}{\hbar}\int_0^t (V_A - V_X)dt'\right), \tag{8}$$

$$\frac{dC_A}{dt} = \frac{d\boldsymbol{Q}}{dt} \cdot \boldsymbol{d}_{XA} C_X \exp\left(\frac{i}{\hbar}\int_0^t (V_A - V_X)dt'\right). \tag{9}$$

C_X and C_A are the (complex) expansion coefficients of the wave packet corresponding to the lower (X) and upper (A) adiabatic surfaces, and $\boldsymbol{Q}$ is the vector of six generalized coordinates. The vector $\boldsymbol{d}_{XA}$ is the nonadiabatic coupling vector, defined in terms of the mixing angle θ as $\boldsymbol{d}_{XA} = \nabla_Q \theta$. The mixing angle, in turn, is defined in terms of the Massey parameter p by

$$\theta = \tan^{-1}[p + (1+p^2)^{1/2}], \tag{10}$$

where

$$p = \frac{2K_{\mathrm{cl}}\hbar}{\mu_r r^2 (V_A - V_X)}; \tag{11}$$

K_{cl} is the component of the classical angular momentum along the H–H axis (with the same units as $\hbar$), r is the H–H distance, and μ_r is the H–H reduced mass. We computed K_{cl} and the components of $\boldsymbol{d}_{XA}$ analytically in terms of the generalized coordinates and momenta of the trajectory program. In the description used here, p is a signed quantity, while in Ref. 24 the absolute value is used; because $(V_A - V_X) \geqslant 0$ everywhere, our definitions are equivalent to Eqs. (18) and (19) of Ref. 24. The electronic propagation occurs independently of which of the two adiabatic surfaces the classical propagation is currently using; we will refer to the "current" state and the "other" state.

At each trajectory step, the time derivative of the quantum population $|C_X|^2$ or $|C_A|^2$ in the other state is evaluated. If the derivative is positive, then a hopping probability is computed according to $P = \dot{a}' \Delta t / a$, where Δt is the time step, a is the quantum population in the current state, and $\dot{a}'$ is the derivative of the population in the other state. A random number ξ in [0,1) is drawn and if $\xi < P$ the trajectory "hops" and begins using the other surface. At such a hop the total energy is conserved by adjusting the momenta along a direction perpendicular to the H–H vector. It is possible that for an upward hop no such adjustment is possible; in that case the hop is called "frustrated" and no switch of surface is made.

In this model, the coupling between the two surfaces and the resulting hopping probability are largest when $|p|$ has a value near 1. Usually $|p| \ll 1$; since K_{cl} is limited by the total angular momentum and r never becomes very small, in this model p makes large excursions only when the two electronic surfaces become nearly degenerate so that $(V_A - V_X)$ becomes small. Degeneracy occurs both at linear configurations and at long range in $N+H_2$ geometries for any angle (Fig. 1). The model, however, cannot be expected to describe the hops in the $N+H_2$ channel accurately; several steps in its derivation require the assumption of near linear geometries. Santoro *et al.*[24] suppressed the hops at long range with an exponential switching function that turned on at $R = 2a_0$, where R is the $N-H_2$ Jacobi distance. (They were studying the $N+H_2$ reaction, so these hops were occurring in the entrance channel.)

We began our study without such a switching function, expecting that hops at $N+H_2$ geometries at distances shorter than the exit barrier would be relatively unimportant, and hops beyond the exit barrier in the $N+H_2$ channel would be irrelevant because trajectories in that asymptotic channel contribute to the same $N(^2D)+H_2$ products no matter which surface is current when the trajectory is terminated. Our initial computational results were very encouraging: we obtained average quenching rates that agreed well with the experimental results. However, a closer inspection showed that about 90% of the hops that contributed to the computed quenching rate were occurring at $N+H_2$ geometries, at all angles, rather than at near linear H–N–H geometries, as we had expected. Suppressing those ill-described hops, either abruptly or with a smooth switching function as used by Santoro *et al.*, would result in a computed quenching rate that was less than 10% of the observed rate.

We then reexamined the derivation of the SPS surface-hopping model[24] and found that in the transition between Eq. (10) and Eq. (11) in Ref. 24 the assumption $K \gg \lambda$, where K is the ordinary dimensionless quantum number representing the projection of the total angular momentum on the H–H axis and λ is the projection quantum number for the electronic angular momentum, was applied in two different ways. At one place in Eq. (10), $-2K^2 - \lambda^2 + 2K\lambda$ was replaced with $-2K^2 + 2K\lambda$; that is, only the second order term with respect to λ was dropped. In another place, Santoro *et al.*[24] replaced $(K-\lambda)^2$ with K^2; that is, they dropped both first and second order terms.

The retained first order term is responsible for all the RT coupling in the model. However, the factor multiplying $(K-\lambda)^2$, namely, $(b_r + B_R)/\sin^2\gamma$, is always larger than the b_r factor multiplying $-2K^2 - \lambda^2 + 2K\lambda$; here, $b_r = (2\mu_r r^2)^{-1}$ and $b_R = (2\mu_R R^2)^{-1}$, and μ_r and μ_R are the reduced masses appropriate for the Jacobi coordinates r and R, respectively. R is the distance from N to the center of mass of H_2 and γ is the $N-H_2$ Jacobi angle, i.e., $\cos\gamma = \vec{R}\cdot\vec{r}/(Rr)$. In other words, the first order term that was dropped in the derivation is always larger than the first order term that was retained. More importantly, the prefactor for the dropped term can become very large, either because B_R diverges as the N atom approaches the H–H center of mass (H–N–H, $R \to 0$) or because $1/\sin^2\gamma$ diverges when the Jacobi angle approaches 0°

or 180° in H–N–H or N–H–H geometries. In contrast, the prefactor for the retained RT coupling term, b_r, does not show a particularly strong variation when linear H–N–H geometries are approached. However, it depends noticeably on the H–H separation and the RT coupling would gradually diminish when r becomes larger. This behavior is implausible because the RT coupling arises from the rotation of N about the H–H axis and should not depend much on the separation of the two H atoms.

We implemented a modified version of the SPS model by retaining both first order terms. The principal change in the resulting model is that the Massey parameter p gains the new definition

$$p = \frac{2K_{\mathrm{cl}}\hbar}{V_A - V_X}\left[\frac{1}{\mu_r r^2} - \frac{1}{\sin^2\gamma}\left(\frac{1}{\mu_r r^2} + \frac{1}{\mu_R R^2}\right)\right]. \tag{12}$$

The computation of the nonadiabatic coupling terms $\boldsymbol{d}_{XA}$ from this new version of p is still straightforward. The stronger coupling in the new model forced us to use a somewhat smaller time step than in the original model to ensure norm conservation, but there were no substantial difficulties.

Unfortunately, the modified model suffers from just as bad a disease as the original: it yields quenching rate coefficients that are much too high. In this model, approximately 96% of the reactive trajectories end up in the $NH(X)+H$ channel, while the experiment shows that only about 35% do (Table I).

The new model probably fails for a fundamental reason. The surface-hopping method computes a hopping probability per unit time along the trajectory. The RT transitions occur near linearity, when the bond angle passes through a maximum during the molecular vibration. For $K\neq 0$ this maximum angle is smaller than 180° because of a centrifugal-type potential proportional to K^2 [Eq. (11) in Ref. 24]; in other words, the molecule never becomes really linear. Since the angle is going through a turning point, it can be expected that the classical trajectories will spend too much time in the region of the maximum; the consequent total hopping probability per bending period will be too large because the trajectories will take too many steps in the region of large hopping probability compared to a quantum mechanical description. The corresponding quantum mechanical distribution function of the bending angle has its maximum not at the classical turning point but at a smaller angle, farther away from linearity where the RT coupling is smaller. Therefore a quantum mechanical model will lead to a smaller transition probability per bending vibration and ultimately to a smaller quenching rate coefficient. Histograms of the distributions of angles along representative trajectories do display the expected maximum near the angular turning point with $\alpha<180°$.

In order to avoid numerical instabilities very near linear geometries, when both K_{cl} and V_A-V_X are approaching zero, Santoro *et al.* used a Gaussian damping function that suppressed the RT coupling when the nitrogen atom came within about $0.1a_0$ of the H–H axis. In our calculations the centrifugal barrier kept the trajectories sufficiently far from linearity that this damping function was not necessary for numerical purposes. It would be possible to use such a damping function to reduce the overall coupling strength and empirically adjust the quenching rate in the modified model to match the experiment. Instead, we chose a different empirical model whose physical interpretation we think is clearer. It is described in the next section.

Defazio and Petrongolo retained the $K\lambda$ term proportional to $B_R/\sin^2\gamma$ in their recent quantum mechanical model.[25] That model, of course, does not suffer from inaccuracies associated with turning point behavior. However, it also showed a much greater influence of RT coupling on the reaction than did the TSH calculation of Santoro *et al.*, consistent with our experience.

B. Empirical model

It is clear that a better, presumably quantum mechanical, method of computing the RT transition rate is required. However, this system has two coupled PESs, each having a deep well, three reaction channels, and high excess energy in two of the channels. Exact quantum calculations are highly demanding, although possible as the recent calculations of Defazio and Petrongolo show.[25] In the present work we adopted an empirical approach. The model makes two assumptions: (i) The probability of a RT transition is the same on each passage near linearity during the molecular vibration, and (ii) once the transition has taken place, the molecule will dissociate on the ground state surface with no further electronic transitions. We then chose a value of the "transition probability per attempt at linearity" P to give good agreement with the observed quenching rate coefficient for the $NH(a)+H$ isotopic variant.

Our empirical model is inspired by the wave packet model of Dixon.[35] He performed two-state wave packet calculations on a model potential surface with a linear upper state and a bent lower state, then fitted the results to an empirical formula that could be used to compute a hopping probability per vibrational period. The model potentials employed by Dixon are not appropriate for NH_2, for which both upper and lower states are bent. Instead, we adopt his general approach. Classical mechanics gives the correct vibrational frequency, even though it gives the wrong distribution of coordinates over a vibrational period. It is therefore reasonable to use classical mechanics to determine the number of times the highly excited NH_2 molecule in the $\tilde{A}$ state passes near linearity per unit time. Unlike the probability of Dixon, our P is independent of energy as well as K; it represents an effective transition probability per period of the bending vibration.

Each time a trajectory passes near linearity, we draw a random number ξ in $[0, 1)$ and compare it to the empirically selected P; if $\xi<P$, then we switch the trajectory to the lower surface, adjust the momenta as described above, and continue the trajectory on the lower surface until the complex dissociates. We consider the trajectory to have passed near linearity if the bond angle α goes through a maximum with a value greater than a critical value α_{crit}, selected to be 120°.

We selected P by choosing it to give the correct fraction of trajectories yielding $NH(X)+H$ at a collision energy of

0.6 kcal/mol with NH(a) in an initial state $j=2$, which is representative of the 298 K thermal distribution in the experiment. The resulting value is $P=0.0051$; that is, about half of 1% of the attempts at linearity result in a RT transition. We then used this value of P in all cross section calculations for all isotope variations.

If many trajectories had maxima near $\alpha=\alpha_{\text{crit}}$, then α_{crit} itself would act as an empirical parameter; however, inspection of representative trajectories indicated that the maxima usually occurred either well below or well above 120°. We tested the insensitivity of our results to the value of α_{crit} by running three sets of trajectories with a collision energy of 0.6 kcal/mol and initial j of 0, 2, and 6, using $\alpha_{\text{crit}}=140°$. The total quenching cross section decreased by merely 4%, 5%, and 7% for the three initial rotational states.

C. Computational details

We modified the three-body trajectory program CLASTR of Muckerman[36] to perform all the calculations described here. Hamilton's equations for the six internal coordinates and their conjugate momenta were solved on either the X or the A PES. For the "Tully-style" calculations, the four equations describing the (complex) electronic amplitudes and the single equation needed to compute the integrated electronic phase were included in the differential equation system for a total of 17 coupled equations.

The potential surfaces are implemented as splines[14] and consequently have discontinuous higher derivatives at the boundaries between spline cells. It is therefore not advantageous to use a high-order method to solve the differential equations. We used the fourth/fifth order adaptive step size Runge-Kutta method implemented in the RKSUITE package.[37] The surface-hopping calculations require many thousands of random deviates, and we used the long-period random number generator of L'Ecuyer and Cote,[38] as implemented in the RANLIB package,[39] to avoid problems of period exhaustion.

The long-lived trajectories are chaotic, and we cannot claim that our trajectory calculations are accurately converged in any strict sense. We exclude from the analysis any trajectories that fail to conserve total energy within one part in 10^5, total angular momentum within one part in 10^8, or (for Tully-style calculations) electronic norm within one part in 10^9. Trajectories on a single electronic surface can be accurately back-propagated only for propagation times less than about 200 fs. We adopt the attitude of Crisanti *et al.*,[40] who argue that small errors in the solution of the equations of motion are equivalent to small displacements in the initial conditions. Since we sample a random distribution of initial conditions and average over the results, we do not expect the errors in our trajectories to affect our computed statistical properties in any physically important way.

We calculated cross sections $\sigma_n(E_c,j_i)=\pi b_{\text{max}}^2(N_n/N_{\text{tot}})$, where n labels one of five product channels indicated in Eq. (3). Here, N_n is the number of trajectories terminating in channel n and N_{tot} is the total number of trajectories for a particular collision energy E_c and initial rotational state j_i. E_c ranges from 0.2 to 14 kcal/mol and j_i ranges from 0 to 16 for NH and to 22 for ND. At each collision energy the maximum impact parameter b_{max} was adjusted to ensure convergence of the cross sections. At least 10 000 trajectories were computed for each energy and initial state.

Thermal rate coefficients for channel n were computed according to

$$k_n(T)=\frac{\eta}{(\pi\mu)^{1/2}}\left(\frac{2}{k_BT}\right)^{3/2}Q^{-1}\sum_{j_i}(2j_i+1)\exp(-E_{j_i}/k_BT)\times\int_0^\infty E_c\sigma(E_c,j_i)\exp(-E_c/k_BT)dE_c, \quad (13)$$

where μ is the reduced mass for the reactant channel, k_B is the Boltzmann constant, Q is the rotational partition function, and E_{j_i} is the initial rotational energy of the diatom. The electronic degeneracy factor η is 1/2 for NH(a)+H. The integral over E_c was performed with the overlapping-parabolas method.[41]

IV. RESULTS

A. Cross sections

Figure 4 shows cross sections for several different product channels as functions of collision energy, for the NH(a)+H isotope combination. The behavior for $j_i=0$ is typical of a complex forming reaction, with cross sections that fall steeply with energy at low energy and then level off. Initial rotational excitation of the diatomic causes a modest dynamical barrier to complex formation. For $j_i=2$ the cross section at the lowest energy (0.2 kcal/mol) is about half as large as for $j_i=0$, and by $j_i=8$ the largest cross sections increase with collision energy below 4 kcal/mol. For all energies and all j_i the cross sections for the N(^2D)+H_2 channel and for the exchange channel are the largest and the cross sections for quenching and quenching plus exchange are the smallest.

Figure 5 shows the same data plotted against j_i. Cross sections into all the product channels fall off similarly with j_i, indicating that initial rotation causes a dynamical barrier to complex formation, but the dynamics within the NH_2 complex is largely independent of the initial rotational state of the diatomic. With increasing collision energy the dependence on j_i becomes weaker.

To assist in studying the complex dynamics, we classify trajectories according to the number of "minimum exchanges" M in the manner of Schlier and Seiter.[42] During the trajectory, we keep track of which atom-atom distance is smallest; each time the shortest distance switches from one pair of atoms to another, we count one minimum exchange. In a long-range collision, the same atom-atom distance will remain the shortest one throughout. In a direct A+BC $\rightarrow$AB+C collision, there will be only one minimum exchange. We define a complex-forming trajectory as one in which there are two or more minimum exchanges.

Figure 6 shows the number of trajectories ending in the four H+NH channels as a function of M; the N+H_2 channel is not shown. Each panel was constructed from a set of 100 000 trajectories, all for $j_i=2$ and $E_c=0.6$ kcal/mol. The horizontal axis roughly corresponds to time, with two minimum exchanges in each full period of the asymmetric stretch

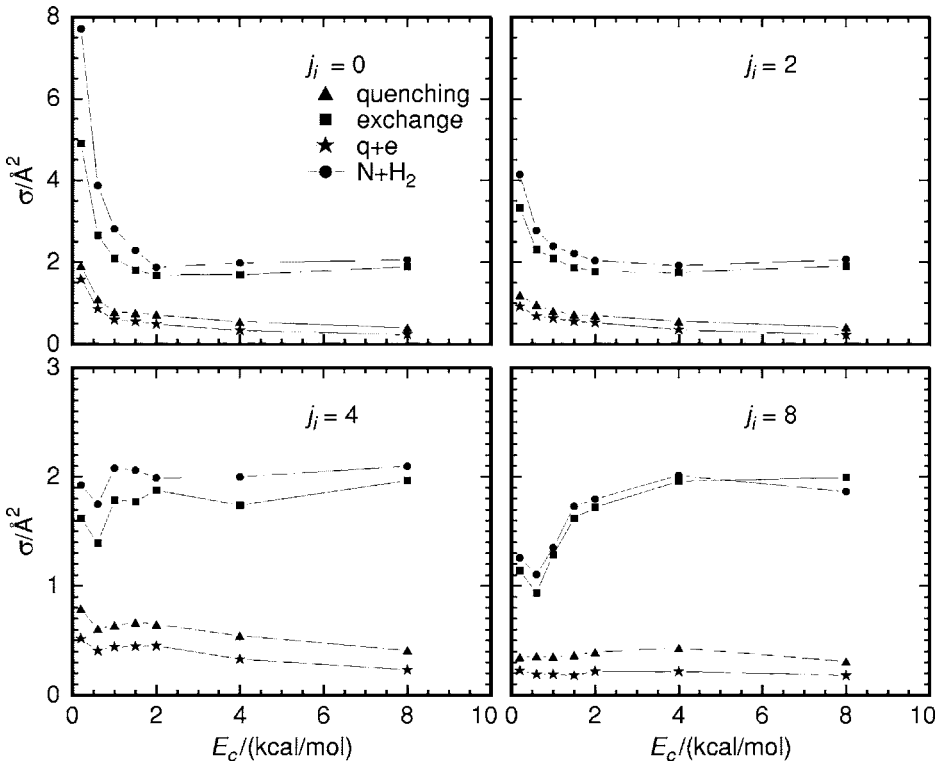

FIG. 4. Cross sections as functions of collision energy E_c for NH(a)+H and four initial rotational states j_i of NH(a).

vibration. For the H+NH combination, about $M=100$ is required before the M distributions for the "no reaction" and "exchange" channels converge. In other words, about 100 minimum exchanges must occur before the complex "forgets" which H atom was the incoming one. The convergence occurs more rapidly, requiring about $M=50$, for D+ND. The distributions for the unsymmetric combinations are biased such that an unsymmetric complex prefers to lose the H atom. D+NH complexes are most likely to lose D for $M \leqslant 80$, but then the curves cross and longer-lived complexes are slightly more likely to lose the H atom. H+ND complexes are at least twice as likely to lose H as D no matter how long they survive. These results show clearly that most complexes dissociate before the realm of statistical behavior has been reached, and strong nonstatistical effects can be expected. This is in accord with the observations made by

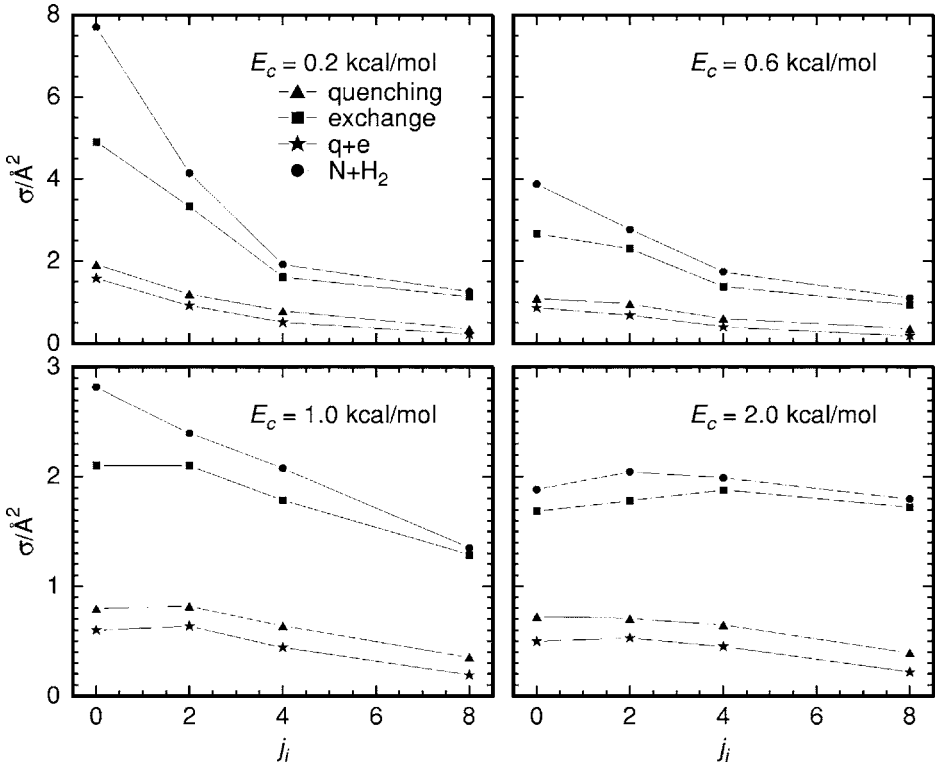

FIG. 5. Cross sections as functions of the initial rotational state of NH(a) for NH(a)+H.

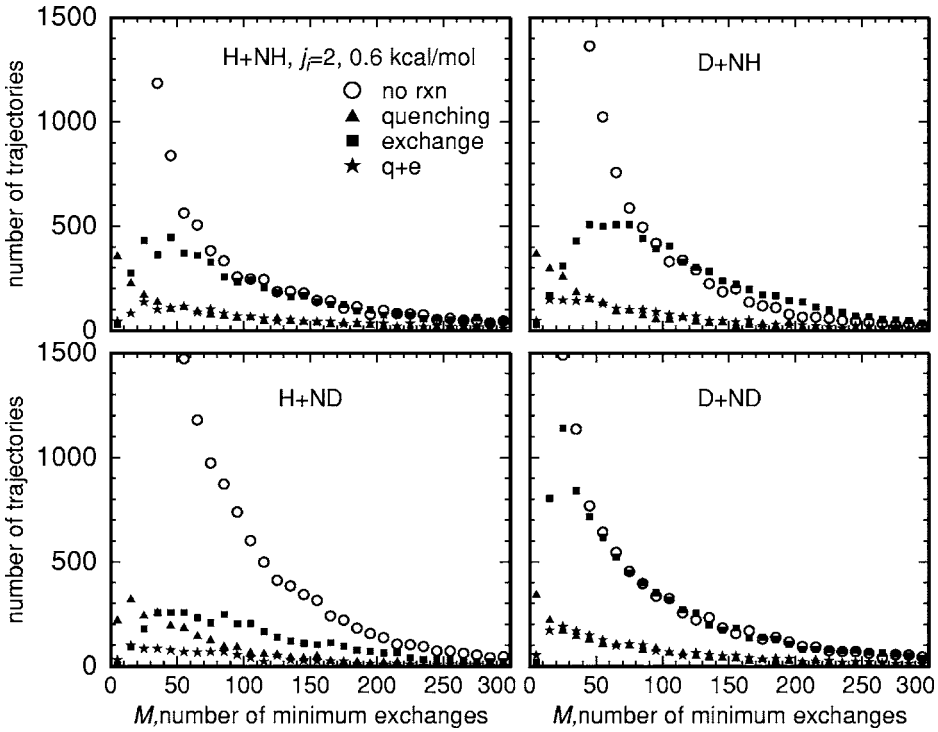

FIG. 6. Number of minimum exchanges M for 100 000 trajectories for each isotope combination.

Qu *et al.*[14] for H+NH reactions in the X state. The data for complexes producing products on the lower surface in Fig. 6 show similar trends, though the "equilibrated" behavior appears much earlier.

Figure 7 shows the variations in cross sections among the different isotope combinations. The lower left panel is the cross section for complex formation σ_{cf}. It is large at small collision energies, quickly decreases to a more or less

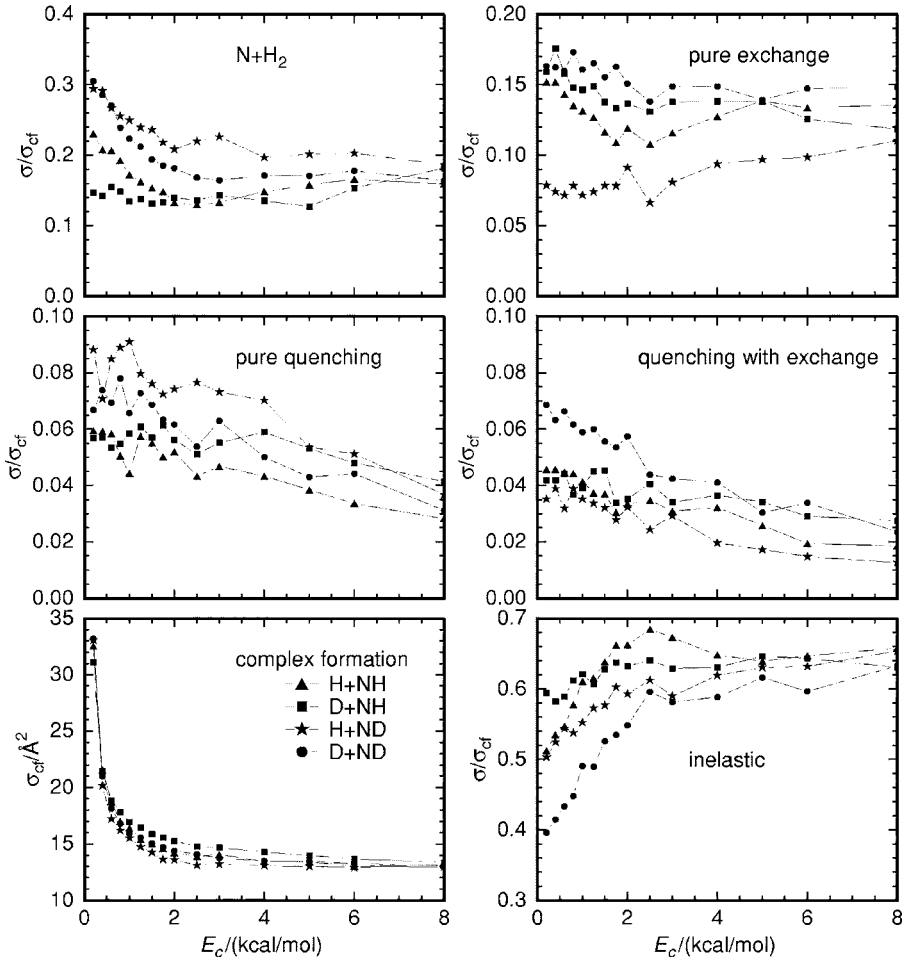

FIG. 7. Cross sections into different product channels expressed as fractions of the complex formation cross section, σ_{cf}, as functions of collision energy. The lower left panel gives the complex formation cross section. The "inelastic" panel excludes non-complex-forming trajectories, so that the sum of all the fractional cross sections is unity.

TABLE II. Computed channel-specific rate coefficients at 298 K, in units of 10^{12} cm^3 mol^{-1} s^{-1}. The notation (q for quenching and e for exchange) corresponds to the rate coefficients of reaction (3). The computed entries in Table I are appropriate sums of these values; for example, for H+NH, the rate coefficient for the production of NH(X) is the sum of the q and $e+q$ entries here.

	$N(^2D)$ (X)	$N(^2D)$ (A)	q	$e+q$	e
H+NH(a)	0.3	17.6	5.8	4.1	14.7
D+NH(a)	0.2	12.5	4.4	3.2	13.4
H+ND(a)	0.4	25.5	8.4	3.3	9.1
D+ND(a)	0.3	16.9	5.3	4.3	14.1

constant value, and shows only a weak isotope dependence. The other panels show the cross sections for other product channels as fractions of σ_{cf}. We treat all five exit channels from the complex separately, whether or not they can be distinguished experimentally for a given isotope combination. The relative inelastic cross section (i.e., fragmentation of the complex into the entrance channel) is largest; it first increases with E_c and then levels off at around 2 kcal/mol. The fractional cross sections for pure exchange and for the $N+H_2$ channel are roughly energy independent. The two quenching cross sections, on the other hand, show a slight decrease with collision energy: As E_c increases, the complex survival time decreases and fewer passages through linearity occur.

B. Thermal rate coefficients

Table II shows the computed rate coefficients into each of the individual product channels at 298 K for all the isotope combinations. The two electronic surfaces become degenerate in the $N(^2D)+H_2$ limit, so the two corresponding channels are experimentally indistinguishable. Nevertheless, the results for the two $N(^2D)$ channels are shown separately to make it clear that most of the trajectories producing $N(^2D)$ remain on the upper surface. The $N+H_2$ channel has the largest rate coefficient for all isotope combinations except D+NH. The ratio of rate constants for this channel following the reactions H+NH and D+NH is approximately $\sqrt{2}\approx 1.4$, as predicted by the prefactor in Eq. (13). The same applies for the reactions H+ND and D+ND. The rate coefficients for the pure exchange channel (e) are slightly smaller than those for the N atom channel. These two processes compete with each other on the A' PES; however, because of the exothermicity of 0.3 eV (measured with respect to the exit channel barriers) the N atom channel is more likely to be populated. The exchange rate coefficients have more or less the same value for all isotope combinations, except the H+ND variant. In this case, the simple $\mu^{-1/2}$ kinetic factor does not describe the variation from H to D in the entrance channel. For example, k^e_{D+NH} is only marginally smaller than k^e_{H+NH} and k^e_{D+ND} is even substantially larger than k^e_{H+ND}. As already discussed by Qu *et al.*[14] for the NH(X)+H exchange reaction on the ground state PES, the fragmentation of the complex is not statistical and the dynamical, i.e., nonstatistical, effects depend strongly on the isotopic constitution.

The quenching rate coefficients are clearly smaller than the rate coefficients for the processes proceeding exclusively on the upper state PES. For the same diatom in the entrance channel, NH or ND, the rate coefficient for H atoms is always larger than for the D atoms, which is in qualitative accord with the mass dependent prefactor in Eq. (13). This indicates that the quenching process does not depend much on the isotope variant. The rate coefficients for quenching combined with exchange show a more complicated isotope dependence, probably for the same reasons as mentioned for the pure exchange reaction.

The rate coefficients for the isotope variant H+ND in Table II differ strikingly from the results for the other mass combinations. This correlates with the observation in Fig. 6 that H+ND is the least statistical (see also Ref. 14 for reactions on the X PES).

In Table I we compare all the measured rate coefficients with the corresponding computed values. We chose our empirical RT transition probability P essentially by matching the quenching rate for the NH(a)+H reaction; this rate is marked (*) in Table I. The experimental total removal rate coefficients are generally more reliable than the channel resolved rate data. For D+NH and H+ND reactions, the pure exchange channel contributes to the total loss rate for NH(a) or ND(a), while for the D+ND and H+NH reactions it does not. This explains, for example, why the computed k_{NH+D} is larger than the computed k_{NH+H} despite the lower collision rate caused by the higher mass of D.

The calculated total removal rate coefficients can be meaningfully compared with experiment for all four isotope combinations. Three of the four agree very well. This good agreement indicates that the $A\,^2A'$ PES and the classical descriptions of complex formation and breakup on the upper surface are reasonably accurate. About a third of the complexes make RT transitions, so severe underestimates in our model of the RT rates would produce disagreements in the total removal rates on the order of 35%. The agreement for three isotope combinations is substantially better, though the experimental error bars are also on the order of 30%. Severe overestimates of the RT rates in the calculation would make the total loss rates much too high.

The fourth isotope combination is NH+D. The measured k_{NH+D} exceeds the computed value by somewhat more than the estimated experimental uncertainty. We do not know the source of this discrepancy. It is not clear what errors in the model would make the computed removal rate for this particular isotope combination worse than the others. The experimental result itself is somewhat surprising. Both NH(a)+D and ND(a)+H collisions form excited NHD complexes, but at different rates. For the total loss rate of NH(a) to be as high or higher than that of ND(a) in those two reactions, the excited complex formed in NH(a)+D must be sufficiently shorter lived to overcome its slower formation rate. The observed similarity of the total loss rates clearly implies nonstatistical behavior in the complexes, but it is of a type that is not captured by the classical trajectories.

Detailed comparisons between computed and measured rate coefficients are possible for the NH(a)+D reaction. The calculation indicates that pure quenching and quenching with exchange are of comparable importance, contributing 13%

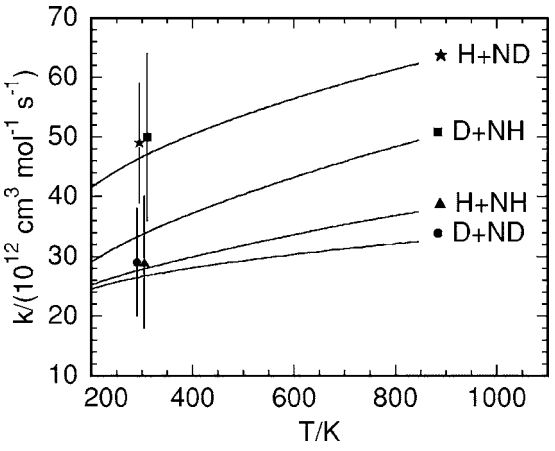

FIG. 8. Measured rate coefficients for loss of NH(a) and ND(a) and corresponding computed values as functions of T. All the experimental measurements are at 298 K; the plotted points have been slightly displaced horizontally for clarity.

and 9% of the total loss rate. The experimental data agree that they are similar in magnitude, though at 17% and 15% they contribute more to the overall loss rate. Our empirical procedure apparently underestimates the rate of RT transitions for the NH(a)+D isotope combination. The calculations also indicate a larger contribution to the total loss rate from pure exchange on the upper surface in the NH(a)+D reaction than the experimental result does.

To make the disagreement for NH+D clearer, we estimate from the data in Table I the rate coefficients for the N atom channel. They are 19 for NH+H and 26 for the reaction NH+D in units of 10^{12} cm^3 mol^{-1} s^{-1}. The corresponding theoretical values are 17.6 and 12.5, respectively. While the agreement is good for the first reaction, the measured rate coefficient for the second one is larger than the calculated value by a factor of 2.

Figure 8 shows computed temperature-dependent total removal rate coefficients for all four isotope combinations and the experimental results at room temperature. The rate coefficients for the removal of NH(a) slightly increase with temperature. The complex formation cross sections displayed in Fig. 7 imply that the increase is due mostly to the increasing collision rate. A similar behavior was observed for the removal of NH(X) by collisions with D on the NHD(X) PES.[14]

V. CONCLUSIONS

Detailed rate constants for the NH($a\,^1\Delta$)+H reaction provide a direct indication of the the effect of the Renner-Teller coupling on the reaction product distribution. The experimental results indicate that about one-third of the collision complexes make a Renner-Teller transition to the ground electronic state of NH_2. The Santoro-Petrongolo-Schatz surface-hopping model was not successful at describing the product branching ratio, in either its original form or our modified one. An empirical model with a single adjustable parameter (the RT transition probability per pass near linearity) chosen for one isotope combination gave results in qualitative agreement with the experiment for all isotope combinations. The agreement was not quantitative for the one isotope combination where detailed comparisons could be made; the experiment yields a larger total removal rate coefficient, a larger fractional contribution of the quenching channels, and a lower fractional contribution of the pure exchange channel than the calculation. The calculations indicate clearly that assumptions of statistical behavior in the collision dynamics are incorrect.

The prediction of the Renner-Teller transition rates from first principles remains to be accomplished. It is clear from this work that either a more sophisticated semiclassical approach or a fully quantum approach will be needed. The recent work of Defazio and Petrongolo[25] appears to offer one tractable possibility.

ACKNOWLEDGMENTS

One of the authors (W.H.) is grateful to Professor Dr. Troe for stimulating interest and financial support and another author (G.C.M.) is grateful to the Max-Planck-Institut für Dynamik und Selbstorganisation for hospitality and support of this work. The authors are indebted to S. Yu. Grebenshchikov for enlightening discussions on the Renner-Teller effect. The authors are also grateful to the Fonds der Chemischen Industrie for financial support.

[1] G. Duxbury, Mol. Spectrosc. (Chem. Soc., London) **3**, 497 (1975).
[2] C. Jungen and A. J. Merer, Mol. Phys. **40**, 1 (1980).
[3] J. M. Brown and F. Jørgensen, Adv. Chem. Phys. **52**, 117 (1982).
[4] K. Dressler and D. A. Ramsay, Philos. Trans. R. Soc. London, Ser. A **251**, 553 (1959).
[5] R. N. Dixon, Mol. Phys. **9**, 357 (1965).
[6] C. Jungen, K.-E. J. Hallin, and A. J. Merer, Mol. Phys. **40**, 25 (1980).
[7] R. N. Dixon, S. J. Irving, J. R. Nightingale, and M. Vervloet, J. Chem. Soc., Faraday Trans. **87**, 2121 (1991).
[8] W. Gabriel, G. Chambaud, P. Rosmus, S. Carter, and N. C. Handy, Mol. Phys. **81**, 1445 (1994).
[9] L. A. Pederson, G. C. Schatz, T.-S. Ho, T. Hollebeek, H. Rabitz, L. B. Harding, and G. Lendvay, J. Chem. Phys. **110**, 9091 (1999).
[10] L. A. Pederson, G. C. Schatz, T. Hollebeek, T.-S. Ho, H. Rabitz, and L. B. Harding, J. Phys. Chem. A **104**, 2301 (2000).
[11] T.-S. Ho, H. Rabitz, F. J. Aoiz, L. Bañares, S. A. Vázquez, and L. B. Harding, J. Chem. Phys. **119**, 3063 (2003).
[12] L. A. Poveda and A. J. C. Varandas, Phys. Chem. Chem. Phys. **7**, 2867 (2005).
[13] L. Adam, W. Hack, H. Zhu, Z.-W. Qu, and R. Schinke, J. Chem. Phys. **122**, 014301 (2005).
[14] Z.-W. Qu, H. Zhu, R. Schinke, L. Adam, and W. Hack, J. Chem. Phys. **122**, 204313 (2005).
[15] M. Alagia, N. Balucani, L. Cartechini, P. Casavecchia *et al.*, J. Chem. Phys. **110**, 8857 (1999).
[16] P. Honvault and J.-M. Launay, J. Chem. Phys. **111**, 6665 (1999).
[17] P. Honvault and J.-M. Launay, Chem. Phys. Lett. **329**, 233 (2000).
[18] N. Balucani, L. Cartechini, G. Capozza, E. Segoloni, P. Casavecchia, G. G. Volpi, F. J. Aoiz, L. Bañares, P. Honvault, and J.-M. Launay, Phys. Rev. Lett. **89**, 013201 (2002).
[19] N. Balucani, P. Casavecchia, L. Bañares, F. J. Aoiz, T. Gonzalez-Lezana, P. Honvault, and J.-M. Launay, J. Phys. Chem. A **110**, 817 (2006).
[20] A. Y. Lin and H. Guo, J. Chem. Phys. **124**, 031101 (2006).
[21] T.-S. Chu, K.-L. Han, and A. J. C. Varandas, J. Phys. Chem. A **110**, 1666 (2006).
[22] T. Suzuki, Y. Shihira, T. Sato, H. Umemoto, and S. Tsunashima, J. Chem. Soc., Faraday Trans. **89**, 995 (1993).
[23] A. J. C. Varandas and L. A. Poveda, Theor. Chem. Acc. **116**, 404 (2006).
[24] F. Santoro, C. Petrongolo, and G. C. Schatz, J. Phys. Chem. A **106**, 8276 (2002).
[25] P. Defazio and C. Petrongolo, J. Chem. Phys. **125**, 064308 (2006).
[26] W. Hack and A. Wilms, J. Phys. Chem. **93**, 3540 (1989).

[27] See EPAPS Document No. E-JCPSA6-126-002702 for the details of the various experiments. This document can be reached via a direct link in the online article's HTML reference section or via the EPAPS homepage (http://www.aip.org/pubservs/epaps.html).
[28] A. Tezaki, S. Okada, and H. Matsui, J. Chem. Phys. **98**, 3876 (1993).
[29] In the "dark" reaction of D atoms with HN_3 only $ND(X)$ but no $NH(X)$ was observed, i.e., the $NH(X)$ concentration was below our detection limit. This observation can be explained by a two step mechanism, $D+HN_3 \rightarrow HD+N_3$ and $D+N_3 \rightarrow ND(X)+N_2$. This is worth mentioning because there is no need to postulate the existence of the radical HN_2. The observation of $NH(X)$ would, however, lead to the conclusion of a reaction $D+HN_3 \rightarrow NH(X)+DN_2$ or $D+HN_3 \rightarrow ND(X)+HN_2$ and thus would give an experimental hint that DN_2 or HN_2, respectively, exist.
[30] J. R. McDonald, J. W. Rabalais, and S. P. McGlynn, J. Chem. Phys. **52**, 1332 (1970).
[31] Á. Vibók, G. J. Halász, S. Suhai, D. K. Hoffman, D. J. Kouri, and M. Baer, J. Chem. Phys. **124**, 024312 (2006).
[32] G. J. Halász, Á. Vibók, R. Baer, and M. Baer, J. Chem. Phys. **125**, 094102 (2006).
[33] T. Takayanagi, Y. Kurosaki, and K. Yokoyama, Chem. Phys. Lett. **321**, 106 (2000).
[34] J. C. Tully, J. Chem. Phys. **93**, 1061 (1990).
[35] R. N. Dixon, Mol. Phys. **54**, 333 (1985).
[36] D. G. Truhlar and J. T. Muckerman, in *Atom-Molecule Collision Theory: A Guide for the Experimentalist*, edited by R. B. Bernstein (Plenum, New York, 1979), Chap. 16, pp. 505–566.
[37] R. W. Brankin, I. Gladwell, and L. F. Shampine, RKSUITE Release 1.0, 1991. (http://netlib.org/ode/rksuite/rksuite.f).
[38] P. L'Ecuyer and S. Cote, ACM Trans. Math. Softw. **17**, 98 (1991).
[39] B. W. Brown, and J. Lovato, RANLIB Library of FORTRAN routines for random number generation, 1991 (http://netlib.org/random).
[40] A. Crisanti, M. Falcioni, and A. Vulpiani, Physica A **160**, 482 (1989).
[41] R. E. Jones, Sandia Laboratories, Technical Report No. SC-M-69–335, 1969 (unpublished). Implemented in the SLATEC program library as subroutine DAVINT (http://netlib.org/slatec).
[42] C. Schlier and A. Seiter, Comput. Phys. Commun. **130**, 176 (2000).